1-1-2009

Ferroelectricity in Ultrathin Strained $BaTiO_3$ Films: Probing the Size Effect by Ultraviolet Raman Spectroscopy

Dmitri Tenne
Boise State University

P. Turner
Boise State University

J. D. Schmidt
Boise State University

M. Biegalski
Pennsylvania State University, University Park

Y. L. Li
Pennsylvania State University, University Park

See next page for additional authors

Ferroelectricity in ultrathin strained $BaTiO_3$ films: probing the size effect by ultraviolet Raman spectroscopy

D. A. Tenne,* P. Turner, and J. D. Schmidt

Department of Physics, Boise State University, 1910 University Dr., Boise, ID 83725-1570

M. Biegalski,† Y. L. Li, L. Q. Chen, A. Soukiassian,‡

S. Trolier-McKinstry, and D. G. Schlom§

Department of Materials Science and Engineering, the Pennsylvania State University, University Park, PA 16802, USA

X. X. Xi

Department of Materials Science and Engineering, the Pennsylvania State University, University Park, PA 16802, USA and Department of Physics, the Pennsylvania State University, University Park, PA 16802

D. D. Fong, P. H. Fuoss, and J. A. Eastman

Materials Science Division, Argonne National Laboratory, Argonne, IL 60439, USA

G. B. Stephenson

Materials Science Division, Argonne National Laboratory, Argonne, IL 60439, USA and Center for Nanoscale Materials, Argonne National Laboratory, Argonne, IL 60439, USA

C. Thompson

Department of Physics, Northern Illinois University, DeKalb, IL 60115

S. K. Streiffer

Center for Nanoscale Materials, Argonne National Laboratory, Argonne, IL 60439, USA

(Dated: September 19, 2009)

Abstract

We demonstrate a dramatic effect of film thickness on the ferroelectric phase transition temperature, T_c, in strained $BaTiO_3$ films grown on $SrTiO_3$ substrates. Using variable temperature ultraviolet Raman spectroscopy enables measuring T_c in films as thin as 1.6 nm, and film thickness variation from 1.6 to 10 nm leads to T_c tuning from 70 to about 925 K. Raman data are consistent with synchrotron x-ray scattering results, which indicate the presence of of 180° domains below T_c, and thermodynamic phase-field model calculations of T_c as a function of thickness.

PACS numbers: 77.84.Dy, 77.80.Bh, 78.30.-j, 63.22.-m

Keywords:

Ferroelectrics, materials possessing a spontaneous and switchable electric polarization, which appears below the Curie temperature T_c, attract a broad interest because of a wide range of their applications, such as non-volatile memory devices or piezoelectric micro- and nanoelectromechanical systems.[1, 2] In recent years, the continuous demand for device miniaturization and advances in epitaxial technology of ferroelectric oxide materials [3, 4] have rapidly moved the the science and technology of ferroelectrics towards thin films and multilayer structures at nanometer scale. Nanoscale ferroelectrics are also fascinating objects from fundamental physics point of view, since reduction of the structural dimensions gives rise to new phenomena and properties dramatically different from those of bulk ferroelectrics.[5–7]

Understanding the basic physics of ultrathin ferroelectric films, in particular, the issue of a critical size for ferroelectricity has been the area of much research effort recently.[5–9] For a long time it was believed that ferroelectricity was suppressed in very small particles and ultrathin films [10, 11], and a spontaneous polarization could not be sustained in a material below a critical size of few tens of nanometers. Later experiments identified a ferroelectric state in much thinner films [12], and recent theoretical work [13, 14] showed the critical size to be much smaller than previously thought. Recent results on $PbTiO_3$ films [8, 15–17] and superlattices [18–22] provided the experimental evidence that ferroelectricity persists down to vanishingly small sizes; it can exist in superlattices containing only one-unit-cell-thick layer of ferroelectric ($PbTiO_3$ or $BaTiO_3$) embedded in much thicker non-ferroelectric $SrTiO_3$. These studies revealed that the issue of critical size is very complex, and electrical and mechanical boundary conditions play an essential role in nanoscale ferroelectricity.[23, 24] In particular, mechanical strain was shown to enhance ferroelectricity in relatively thick ($\geq$50 nm) $BaTiO_3$ films.[25]

Shrinking dimensions demand characterization techniques capable of probing the properties of nanoscale ferroelectrics. Particularly, measuring the Curie temperature T_c in such systems has been difficult, and the T_c information is missing in many reports of ferroelectricity in ultrathin films. Fong *et al.*[17] determined T_c in ultrathin $PbTiO_3$ films by high-resolution synchrotron x-ray scattering. A fundamental property of ferroelectrics that changes qualitatively during the phase transition is the dynamics of lattice vibrations.[10] Thus, its temperature dependence probed by Raman spectroscopy allows determining T_c. Conventional (visible) Raman measurements of oxide thin films and nanostructures are prac-

tically impossible because of the film transparency and small thickness leading to extremely weak Raman signals from thin films and the dominance of a substrate signal. We have demonstrated that ultraviolet (UV) excitation above the bandgap of ferroelectrics such as $SrTiO_3$ and $BaTiO_3$ enabled phonons of nanoscale $BaTiO_3/SrTiO_3$ superlattices to be observed in Raman spectra.[21] Motivated by the lack of experimental data on T_c in ultrathin films, here we focus on the size effect on T_c in strained $BaTiO_3$ films. We report UV Raman scattering in $BaTiO_3$ films as thin as 4 unit cells. Raman results, supported by synchrotron x-ray scattering and thermodynamic phase-field modeling, demonstrate tuning of T_c by over 850 K.

A series of epitaxial (001) $BaTiO_3$ films with thicknesses of 1.6, 2, 2.4, 4, and 10 nm (4, 5, 6, 10, and 25 unit cells) has been grown by molecular-beam epitaxy on TiO_2-terminated (001) $SrTiO_3$ substrates.[3, 25] The growth was monitored by reflection high energy electron diffraction. We have studied both uncapped $BaTiO_3$ films and films of the same thicknesses capped with 10 nm of $SrTiO_3$. The samples have been studied by synchrotron X-ray scattering using the Advanced Photon Source at Argonne National Laboratory. According to x-ray scattering data, all samples except for the 10 nm-thick ones were commensurate to the $SrTiO_3$ substrates, which implies 2.2% biaxial compressive strain in the $BaTiO_3$ films. In the 10 nm film, slight strain relaxation (less than 0.5% of the $BaTiO_3$ volume) occurred.

Raman spectra have been recorded using a Jobin Yvon T64000 triple spectrometer with a liquid-N_2-cooled multichannel CCD detector. For excitation, a 325 nm He-Cd laser line was used with a power density of $0.6\,W/mm^2$ at the sample surface, low enough to avoid any noticeable local heating.[26] Spectra have been measured over a temperature range 10–950 K using a variable temperature closed cycle He cryostat in the range 10–600 K and an evacuated hot stage for the measurements above 600 K.

Fig. 1 shows the spectra of four $BaTiO_3$ films at 295 K compared to that of a bare $SrTiO_3$ substrate. We have measured backscattering spectra in both $z(x,x)\overline{z}$ and $z(x,y)\overline{z}$ polarization configurations and found that the polarized signal dominates the spectra, while almost no signal was observed in $z(x,y)\overline{z}$ geometry. The $BaTiO_3$ films studied were too thin to absorb the UV light completely, and all spectra contain broad second-order Raman features of $SrTiO_3$ substrates in the ranges 200–500 and 600-750 cm^{-1}.[27] In the 10, 5, and 2.4 nm films, the first-order Raman peaks of $BaTiO_3$ are seen, indicating that the films are polar at room temperature. Thinner, 2 and 1.6 nm $BaTiO_3$ films become polar at low temperatures,

$\sim$60–70 K. The inset shows the 10 K spectra of the 1.6 nm film, bare substrate, and the difference spectrum, clearly indicating the presence of $BaTiO_3$ peaks.

For identification of the observed phonon peaks, we compared Raman spectra of the films with the spectra of bulk and thin film $BaTiO_3$[28–30], The most distinct lines due to the phonons of $BaTiO_3$ films were observed at about 175–185, 475, and 540 cm^{-1}, and attributed to TO_1+LO_1, LO_2, and TO_3 modes of A_1 symmetry, respectively.[28, 29] According to the selection rules, the A_1(LO) modes are active in $z(x,x)\overline{z}$ geometry. The presence of the A_1(TO) modes is likely due to deviations from true backscattering along (001) direction. Higher TO_3 phonon frequency in thin films ($\sim$540 cm^{-1}) compared to bulk $BaTiO_3$ ($\sim$522 cm^{-1}), is likely due to the compressive strain. A peak at $\sim$290 cm^{-1} seen in the spectra of the 10 nm $BaTiO_3$ film corresponds to the $A_1(TO_2)$ mode of the tetragonal $BaTiO_3$.[28, 30] This peak overlaps, however, with the substrate features and cannot be distinguished in thinner films, so it was not used in our analysis. $BaTiO_3$ phonon peaks at positions similar to the above described features are characteristic of the spectra of bulk tetragonal $BaTiO_3$[28, 30] and $BaTiO_3/SrTiO_3$ superlattices.[21] Therefore we conclude that $BaTiO_3$ layers are tetragonal in these strained films.

Temperature-dependent Raman spectra for the 2.4 nm-thick $BaTiO_3$ film are shown in Fig. 2. Other films exhibit similar temperature evolution. Bulk $BaTiO_3$ is cubic and paraelectric above T_c=403 K, becomes tetragonal and ferroelectric below T_c, and goes through additional transitions to orthorhombic at 278 K and rhombohedral at 183 K. [31] Each of the three ferroelectric phases can be identified by Raman spectra.[30] In our films, the peak positions and lineshapes remain nearly unchanged with increasing temperature (Fig. 2). Hence, the films remain in the single ferroelectric phase and the low-temperature phases characteristic for bulk $BaTiO_3$ are suppressed. Biaxial compressive strain in our films, which stabilizes the tetragonal c phase, is the cause for such a behavior, also observed in $BaTiO_3/SrTiO_3$ superlattices.[21]

Raman spectra measured as a function of temperature allow T_c to be determined, based on the fact that centrosymmetric perovskite-type crystals have no first-order Raman active modes in paraelectric phase. Above T_c the spectra contain only the broad second order substrate features. Therefore, by plotting the first-order Raman intensity as a function of temperature, T_c can be determined as the temperature where the intensity becomes zero.[21], as illustrated in the inset to Fig. 2 for two of the films studied. We used the A_1(TO_1+LO_1)

and $A_1(TO_3)$ peaks (marked in Fig.2) since they do not overlap with the second-order features. The intensities are normalized by the Bose factor $n+1 = (1 - exp(-\hbar\omega/kT))^{-1}$ ($\hbar$, k, ω, and T are the Planck's and Boltzmann's constants, the phonon frequency, and temperature, respectively), and divided by the intensity of the corresponding mode at 10 K. Both phonon peaks show similar behaviors and the dashed-dotted lines are averages of the linear fits for the intensities of these two modes. (The linear fit corresponds to a parabolic decrease of polarization with temperature as Raman intensity is proportional to the square of atomic displacement.) T_c is determined as the intersection of a dash-dotted line with the horizontal axis.

Raman data show that T_c varies in a very broad range as a function of film thickness, being as high as 925 K for the 10-nm $BaTiO_3$ films. Even the 10 nm-thick films are still nearly fully strained (less than 0.5% of film volume is relaxed, as follows from x-ray scattering data). Fig. 3 summarizes the results of the T_c determination for all the samples as a function of $BaTiO_3$ film thickness. Even the films containing only four monolayers of $BaTiO_3$, are ferroelectric with T_c ~70 K. T_c increases dramatically with increasing $BaTiO_3$ thickness, provided that the films remain fully (or nearly fully) strained.

Synchrotron x-ray scattering results indicate the presence of 180° domains in the 2.4, 4.0, and 10 nm-thick $BaTiO_3$ films capped with 10 nm $SrTiO_3$. Similar to the results obtained for $PbTiO_3$ films,[8, 32] diffuse intensity induced by the periodic nature of the ferroelectric 180° domains appears in the scattering around the $BaTiO_3$ Bragg peaks, as illustrated by the in-plane reciprocal space map for the 10-nm-thick capped film (Fig. 4). While the diffuse intensity was absent at 950 K, it was present at 870 K and below, yielding a T_c value consistent with Raman results. Similar diffuse scattering was observed for the 4 and 2.4 nm capped samples at room temperature. Results on the 2 and 1.6 nm films, however, provided no evidence for diffuse scattering, suggesting that T_c is below room temperature for these films, also consistent with T_c's obtained from Raman data (Fig. 3).

From the reciprocal space maps, the 180° domain period can be determined as the inverse distance from the center to the diffuse intensity maximum along the $\langle 110 \rangle$ direction. For 10 nm sample (Fig. 4), the period is ~6.3 nm. The domain size decreases with film thickness and increases with cooling. While the satellites were not clearly observed for the uncapped $BaTiO_3$ samples, this may be due to the existence of non-periodic domains or domain periods larger than observable by the experimental resolution (~80 nm). Raman spectra and their

temperature evolution for uncapped and capped $BaTiO_3$ films show almost no difference in terms of the shape and relative intensity of phonon peaks. The values of T_c are pretty close for capped and uncapped films of the same $BaTiO_3$ thickness, being slightly higher for capped films.

Observed T_c for the 10-nm films (925 K) approaches the value obtained from the phase diagram calculated without considering the finite thickness effect [33] at the relevant strain, -2.2% ($\sim$1000 K). For thinner films the size effect becomes significant and causes a dramatic decrease in T_c (Fig. 3). Using the phase-field method, we have calculated T_c of $BaTiO_3$ films clamped to $SrTiO_3$ substrates as a function of film thickness. The time-dependent Ginzburg-Landau equations (see Eq. 1 in ref. [33]) have been used, considering surface polarization extrapolation and open circuit electrostatic boundary conditions, corresponding to our case of the films with no electrodes. The bulk Landau energy coefficients, elastic stiffness, and electrostrictive coefficients have been chosen the same as those listed by Li *et al.* [33, 34] The result, shown in Fig. 3, agrees very well with experimental data. Simulations also show the films to consist of 180° tetragonal domains with polarizations pointing up and down normal to the film plane; the domain width increases with the film thickness (at 295 K: $\sim$2–3, 5–6, and 10 nm for 4, 8 and 12 nm-thick films, respectively), in reasonable agreement with x-ray scattering results.

Fong *et al.* [17] observed a different behavior in synchrotron x-ray scattering study of ultrathin tetragonal $PbTiO_3$ films: relatively small suppression of T_c (even for the 1.2 nm film), and no 180° domains formed. The difference can be explained by the fact that the $PbTiO_3$ films studied by Fong *et al.* were grown on conducting $SrRuO_3$ layers and with surfaces exposed to a vapor environment of MOCVD chamber (including oxygen). Therefore, there were free charges available at both interfaces to compensate the depolarizing field. Our $BaTiO_3$ films neither have conducting layers at the bottom interfaces nor free ions in the environment of the top surface, so the size (depolarizing field) effect is more pronounced here.

Comparing our results with other calculations of the phase diagrams of ultrathin $BaTiO_3$ films for ideal short-circuit electrical conditions,[35, 36], films with imperfect-screening metal electrodes [35], and under open-circuit conditions [37], we found a good agreement with the latter calculations. (The T_c value for 2.4-nm $BaTiO_3$ films is 370 K from our Raman data and $\sim$380 K from Fig. 3 of Ref.[37], extrapolated to -2.2% strain). Calculations assuming

unscreened [37] or incompletely screened [38]) depolarizing field also predict the existence of 180° domains, which we have observed in capped $BaTiO_3$ films.

In summary, ultraviolet Raman spectroscopy was applied to study ultrathin $BaTiO_3$ films, commensurately grown on $SrTiO_3$ substrates. Raman scattering from $BaTiO_3$ films as thin as 1.6 nm has been observed, indicating the spontaneous polarization. Variable-temperature Raman spectroscopy demonstrates that interplay between strain and film thickness allows tuning the Curie temperature in a very broad range. T_c as high as ∼925 K was observed in 10-nm films, which is over 500 K above the bulk $BaTiO_3$ value. Raman data are consistent with synchrotron x-ray scattering results. The measured T_c values agree well with thermodynamic phase field model calculations for 2.2% compressively strained $BaTiO_3$ under open circuit boundary conditions.

This work was supported in part by the NSF grants DMR-0705127 (Tenne) DMR-0507146 (Chen, Schlom, Xi), and DMR-0820404 (Chen, Li, Schlom, Xi); US DOE grant DE-FG02-01ER45907 (Xi), DOE EPSCoR grant DE-FG02-04ER46142 (Tenne), and Research Corporation for Science Advancement grant 7134 (Tenne). X-ray studies were performed at the Advanced Photon Source beam line 12ID-D, supported by UChicago Argonne, LLC, Operator of Argonne National Laboratory. Argonne, a US DOE Office of Science Laboratory, is operated under Contract No. DE-AC02-06CH11357.

---

* Electronic address: dmitritenne@boisestate.edu

† Currently at Oak Ridge National Lab., Oak Ridge, TN

‡ Currently at Swiss Federal Institute of Technology (EPFL), Lausanne, Switzerland

§ Currently at Cornell University, Ithaca, NY

[1] J. F. Scott, Science **315**, 954 (2007).

[2] M. Dawber, K. M. Rabe, and J. F. Scott, Rev. Mod. Phys. **77**, 1083 (2005).

[3] D. G. Schlom, *et al.*, Mater. Sci. Eng. B **87**, 282 (2001).

[4] A.-B. Posadas, *et al.*, in *Physics of Ferroelectrics: A Modern Perspective*, edited by K. M. Rabe, C. H. Ahn, and J.-M. Triscone (Springer, Berlin, 2007), p. 219.

[5] C. H. Ahn, K. M. Rabe, and J.-M. Triscone, Science **303**, 488 (2004).

[6] A. Rüdiger, *et al.*, Appl. Phys. A **80**, 1247 (2005).

[7] C. Lichtensteiger, M. Dawber, and J.-M. Triscone, in *Physics of Ferroelectrics: A Modern Perspective*, edited by K. M. Rabe, C. H. Ahn, and J.-M. Triscone (Springer, Berlin, 2007), p. 305.

[8] D. D. Fong, *et al.*, Science **304**, 1650 (2004).

[9] N. A. Spaldin, Science **304**, 1606 (2004).

[10] M. E. Lines and A. M. Glass, *Principles and Applications of Ferroelectrics and Related Materials* (Oxford University Press, New York 1977).

[11] S. Li, *et al.*, Phys. Lett. A **212**, 341 (1996).

[12] T. Tybell, C. H. Ahn, and J.-M. Triscone, Appl. Phys. Lett. **75**, 856 (1999).

[13] J. Junquera and P. Ghosez, Nature **422**, 506 (2003).

[14] N. Sai, A. M. Kolpak, and A. M. Rappe, Phys. Rev. B **72**, 020101(R) (2005).

[15] C. Lichtensteiger, *et al.*, Phys. Rev. Lett. **94**, 047603 (2005).

[16] L. Despont, *et al.*, Phys. Rev. B **73**, 094110 (2006).

[17] D. D. Fong, *et al.*, Phys. Rev. Lett. **96**, 127601 (2006).

[18] M. Dawber, *et al.*, Phys. Rev. Lett. **95**, 177601 (2005).

[19] M. Dawber, *et al.*, Adv. Mater. **19**, 4153 (2007).

[20] H. N. Lee, *et al.*, Nature **433**, 395 (2005).

[21] D. A. Tenne, *et al.*, Science **313**, 1614 (2006).

[22] E. Bousquet, *et al.*, Nature **452**, 732 (2008).

[23] M. Dawber, *et al.*, Phase Transitions, **81**, 623 (2008).

[24] M. Dawber, C. Lichtensteiger, and J.-M. Triscone, J. Phys. Condens. Matter **20** 264015 (2008).

[25] K. J. Choi, *et al.*, Science **306**, 1005 (2004).

[26] see Supporting Online Material for Tenne *et al.* [21].

[27] W. G. Nilsen and J. G. Skinner, J. Chem. Phys. **48**, 2240 (1968).

[28] A. Scalabrin, *et al.*, Phys. Status Solidi B **79**, 731 (1977).

[29] J. D. Freire and R. S. Katiyar, Phys. Rev. B **37**, 2074 (1988).

[30] D. A. Tenne, *et al.*, Phys. Rev. B **69**, 174101 (2004).

[31] *Landolt-Börnstein: Numerical Data and Functional Relationships in Science and Technology, New Series. Group III, Volume 36, Subvolume A1*, edited by Y. Shiozaki, E. Nakamura and T. Mitsui (Springer, Berlin, 2001), p. 67.

[32] S. K. Streiffer, *et al.*, Phys. Rev. Lett. **89**, 067601 (2002).

[33] Y. L. Li and L. Q. Chen, Appl. Phys. Lett. **88**, 072905 (2006).

[34] Y. L. Li, L. E. Cross, and L. Q. Chen, J. Appl. Phys. **98**, 064101 (2005).

[35] B.-K. Lai, *et al.*, Appl. Phys. Lett. **86**, 132904 (2005).

[36] J. Paul, *et al.*, Phys. Rev. Lett. **99**, 077601 (2007).

[37] J. Yu, *et al.*, J. Phys.: Condens. Matter **20**, 135203 (2008).

[38] B.-K. Lai, *et al.*, Phys. Rev. B **75**, 085412 (2007).

FIGURE CAPTIONS

FIG. 1: (Color online) Room temperature Raman spectra of four $BaTiO_3$ ultrathin films on $SrTiO_3$ substrates compared to the spectrum of a bare substrate. Arrows mark the phonon peaks of the $BaTiO_3$ films. The inset shows Raman spectra of 1.6 nm-thick $BaTiO_3$ film and $SrTiO_3$ substrate measured at 10 K, and the difference between the two spectra.

FIG. 2: (Color online) Temperature evolution of Raman spectra of a 2.4 nm-thick $BaTiO_3$ film on a $SrTiO_3$ substrate. Arrows mark the phonon peaks of the film used for T_c determination. The inset shows the temperature dependencies of normalized Raman intensities of the peaks at ∼180 and 540 cm^{-1} ($A_1(TO_1+LO_1)$ and $A_1(TO_3$ phonons, respectively), for 2.4 and 10 nm-thick $BaTiO_3$ films capped with 10 nm $SrTiO_3$ The dashed-dotted lines are fits to a linear temperature dependence.

FIG. 3: (Color online) T_c as a function of the $BaTiO_3$ layer thickness, as determined from Raman data for all films studied (symbols). The dashed-dotted line is a result of the phase-field model calculation with open circuit boundary conditions.

FIG. 4: (Color) In-plane reciprocal space map around the $BaTiO_3$ 303 peak at 500 K for a 10-nm-thick $BaTiO_3$ film capped with 10 nm of $SrTiO_3$. A redder hue indicates higher intensity (log scale). The reciprocal lattice units (rlu) are in terms of the $SrTiO_3$ substrate.

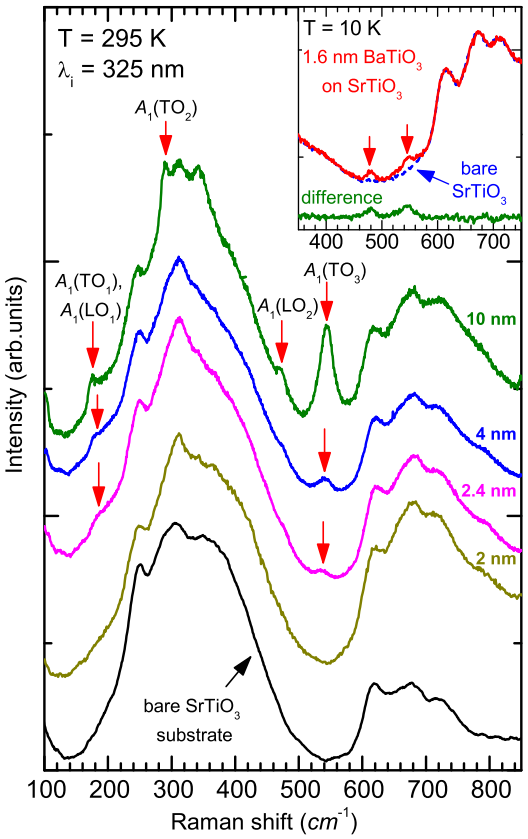

Figure 1
LF12579 *D. A. Tenne et al.*
"Ferroelectricity in ultrathin strained $BaTiO_3$ films"
Physical Review Letters

Figure 1 LF12579 29Sep2009

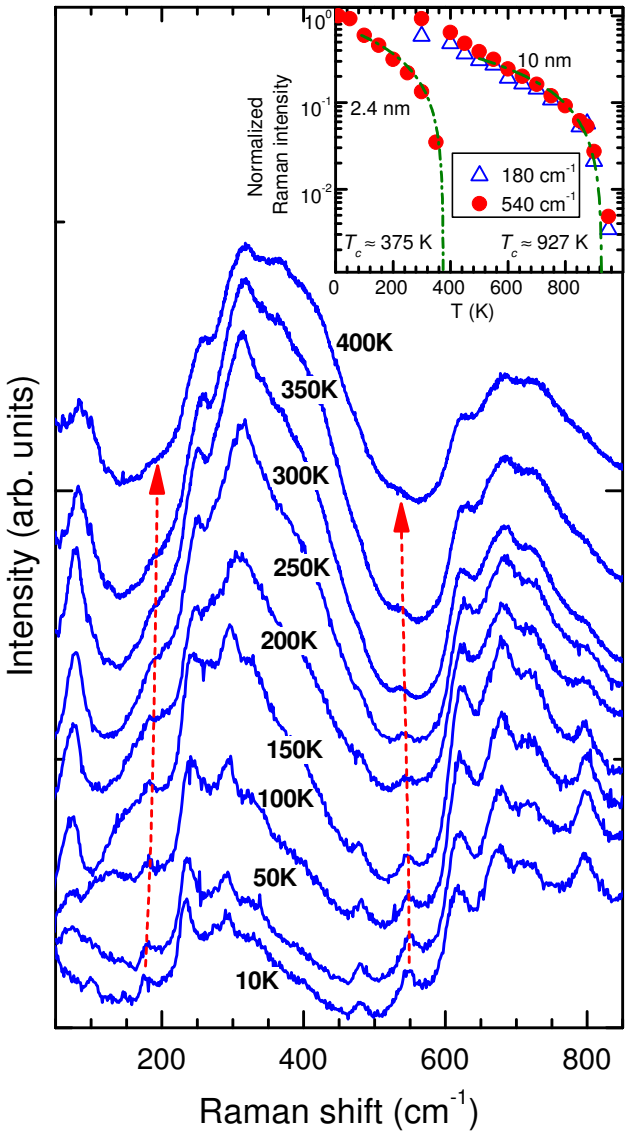

Figure 2

LF12579 *D. A. Tenne et al.*

"Ferroelectricity in ultrathin strained $BaTiO_3$ films"

Physical Review Letters

Figure 2 LF12579 29Sep2009

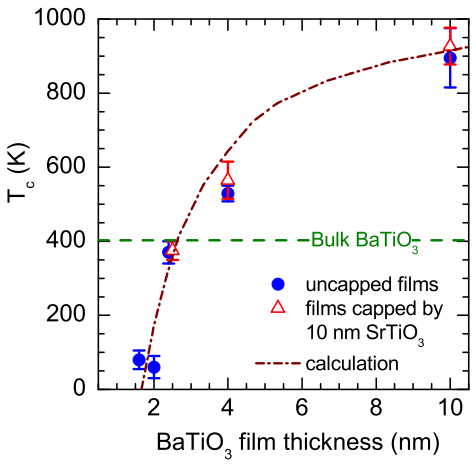

Figure 3
D. A. Tenne et al.
"Ferroelectricity in ultrathin strained $BaTiO_3$ films"
Physical Review Letters

Figure 3 LF12579 29Sep2009

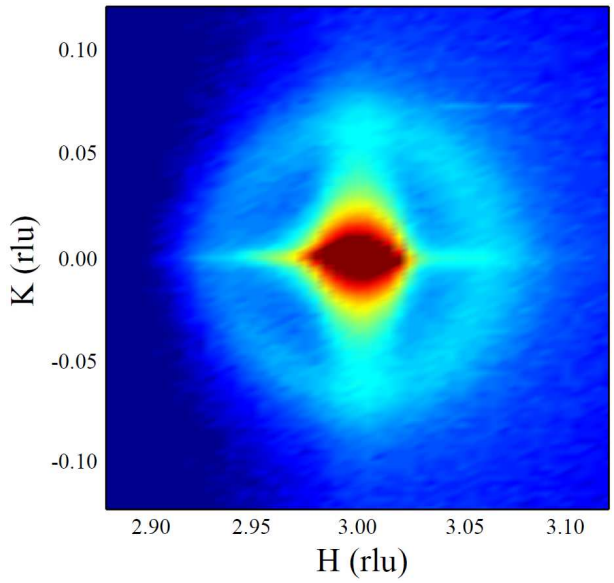

Figure 4
D. A. Tenne et al.
"Ferroelectricity in ultrathin strained BaTiO3 films"
Physical Review Letters

Figure 4 LF12579 29Sep2009